Supporting Information

Adjusted photovoltaic performance of big fused ring-based small molecules by tailoring with different modifications

Min Li [ab]*, Manjun Xiao [c], Zuojia Li [a]*

[a]*Jiangxi Province Key Laboratory of Polymer Micro/Nano Manufacturing and Devices, School of Chemistry, Biology and Materials Science, East China University of Technology, Nanchang 330013, P. R. China*

[b]*School of Materials Science and Engineering, Jiangsu Engineering Laboratory of Light-Electricity-Heat Energy-Converting Materials and Applications, Jiangsu Collaborative Innovation Center of Photovoltaic Science and Engineering, National Experimental Demonstration Center for Materials Science and Engineering, Changzhou University, Changzhou 213164, China.*

[c]*College of Chemistry, Key Lab of Environment-Friendly Chemistry and Application in the Ministry of Education, Xiangtan University, Xiangtan 411105, China.*

Email addresses:

(M.L) limin20a@126.com

(M. X) xmj0704@163.com

(Z. L) lzjshihaoren@126.com

Contents

1. Characterization and Measurement

Nuclear magnetic resonance (NMR) spectra were recorded on a Bruker AV-400 spectrometer using tetramethylsilane (TMS) as a reference in deuterated chloroform solution at 298 K. Mass spectrometric measurements were performed on Bruker Bifiex III MALDI-TOF. Thermogravimetric analyses (TGA) were conducted under a dry nitrogen gas flow at a heating rate of 20 ˚C min^{-1} on a Perkin-Elmer TGA 7. Differential scan calorimetry (DSC) measurements were carried out with a Netzsch DSC-204 under N_2 flow at heating and cooling rates of 10 °C min^{-1}. UV-Vis absorption spectra were recorded on a HP-8453 UV visible system. Cyclic voltammograms (CV) were carried out on a CHI660A electrochemical work station with a three electrode electrochemical cell in a 0.1 M tetrabutylammonium hexafluorophosphate ($TBAPF_6$) acetonitrile solution with a scan 100 mV s^{-1} at room temperature (RT) under argon atmosphere. In this three-electrode cell, a platinum rod, platinum wire and Ag/AgCl electrode were used as a working electrode, counter electrode and reference electrode, respectively. The HOMO and LUMO distributions of SMs were calculated by the density functional theory (DFT) (B3LYP; 6-31G*) method.

2. [1] H NMR and [13] C NMR Spectra

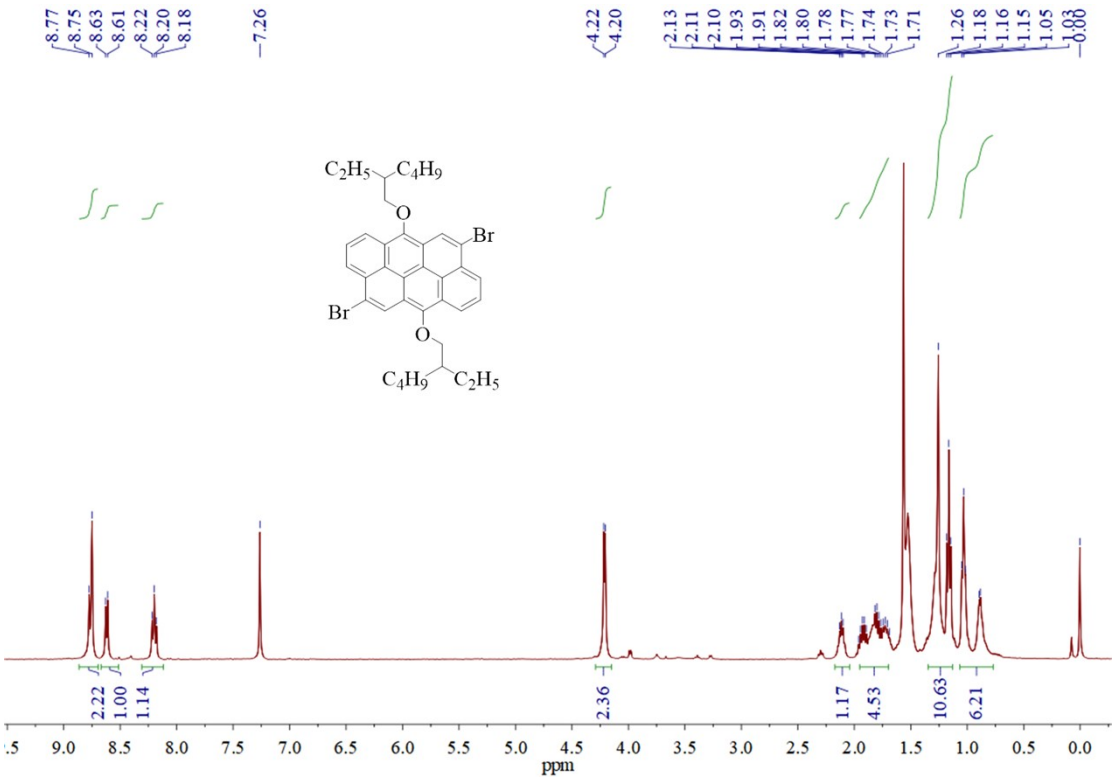

Fig.S1. [1]H NMR spectrum of AAN.

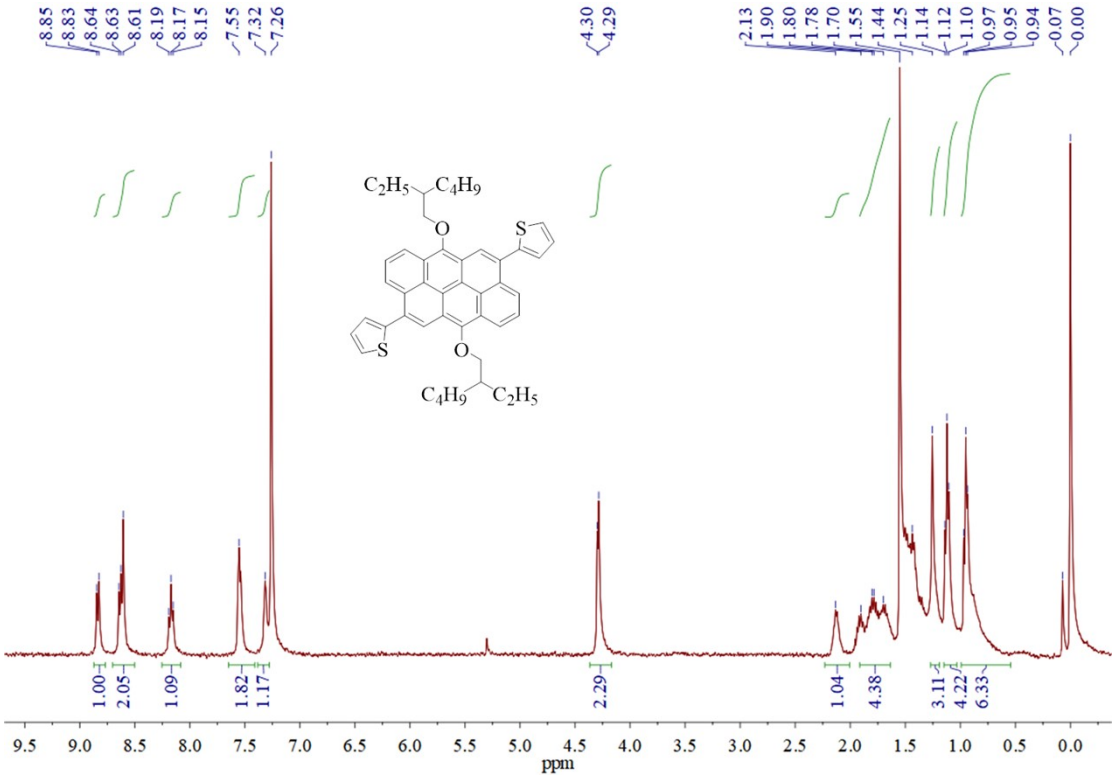

Fig. S2. ^{1}H NMR spectrum of AAN-T.

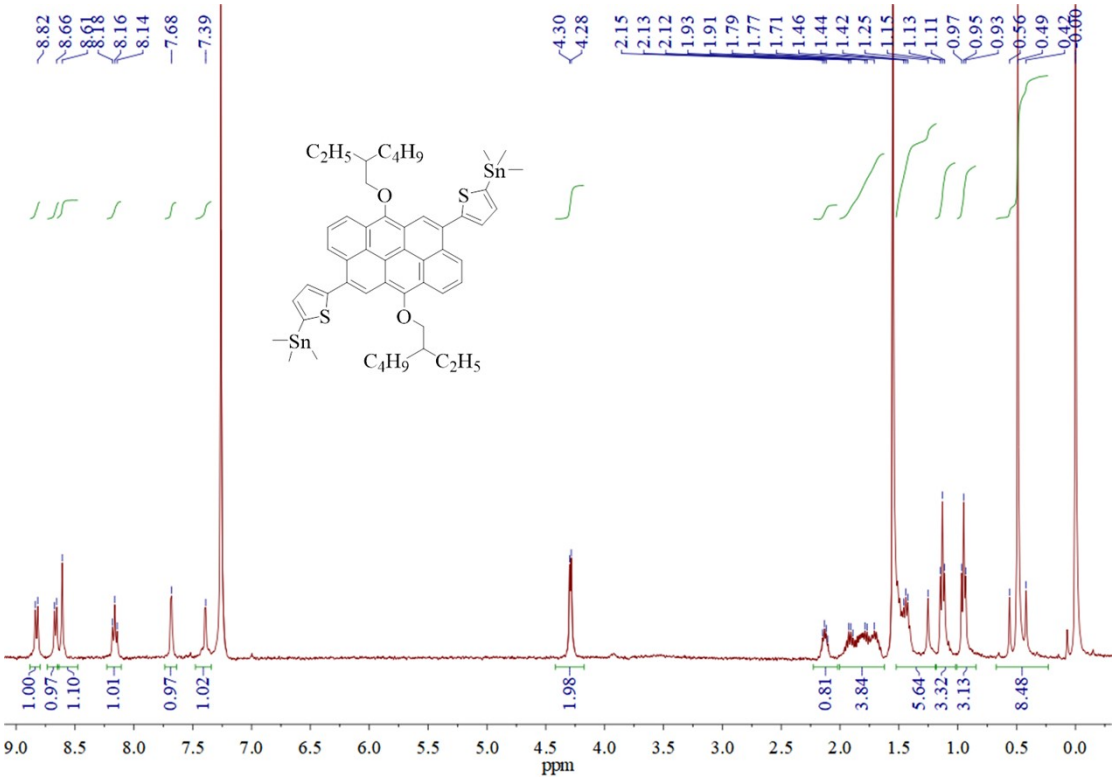

Fig.S3. ^{1}H NMR spectrum of AAN-T-Sn.

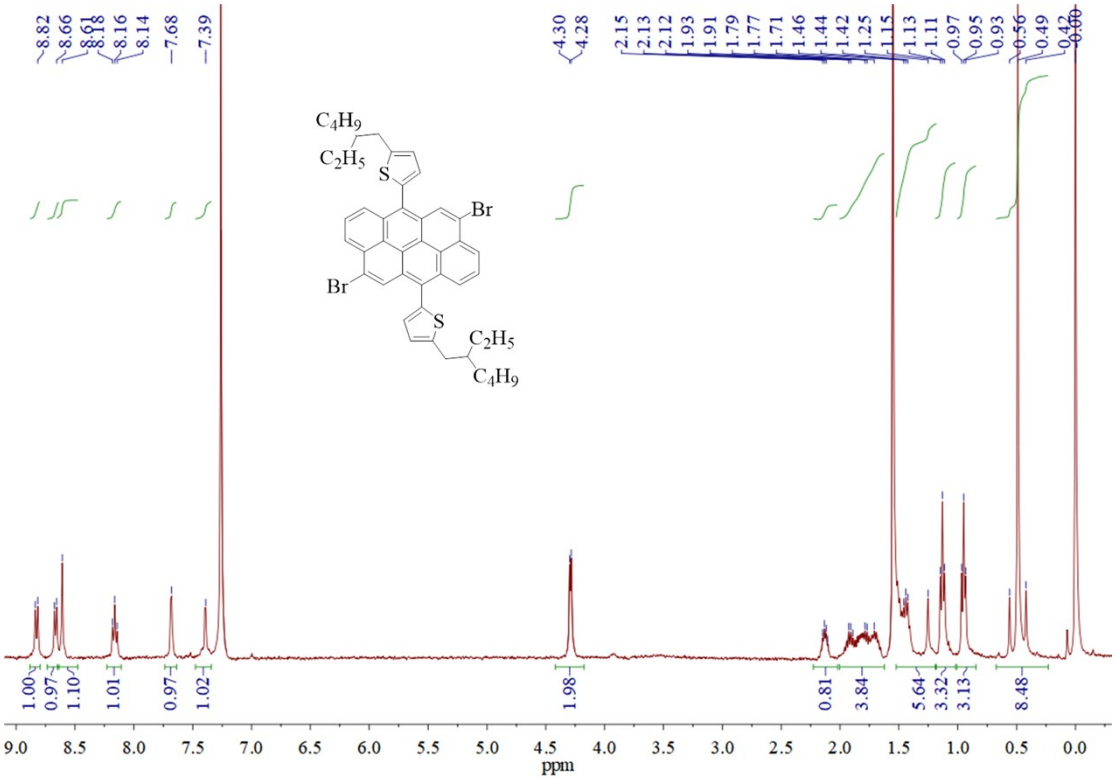

Fig.S4. ^{1}H NMR spectrum of AANT.

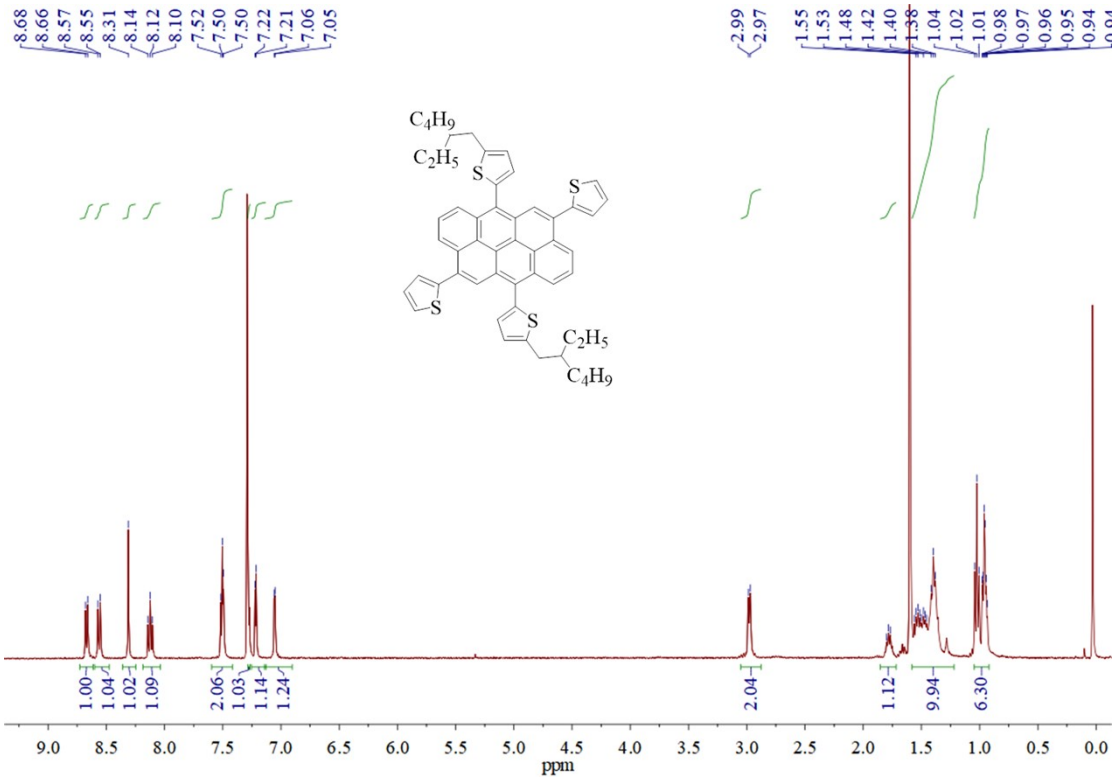

Fig.S5. [1]H NMR spectrum of AANT-T.

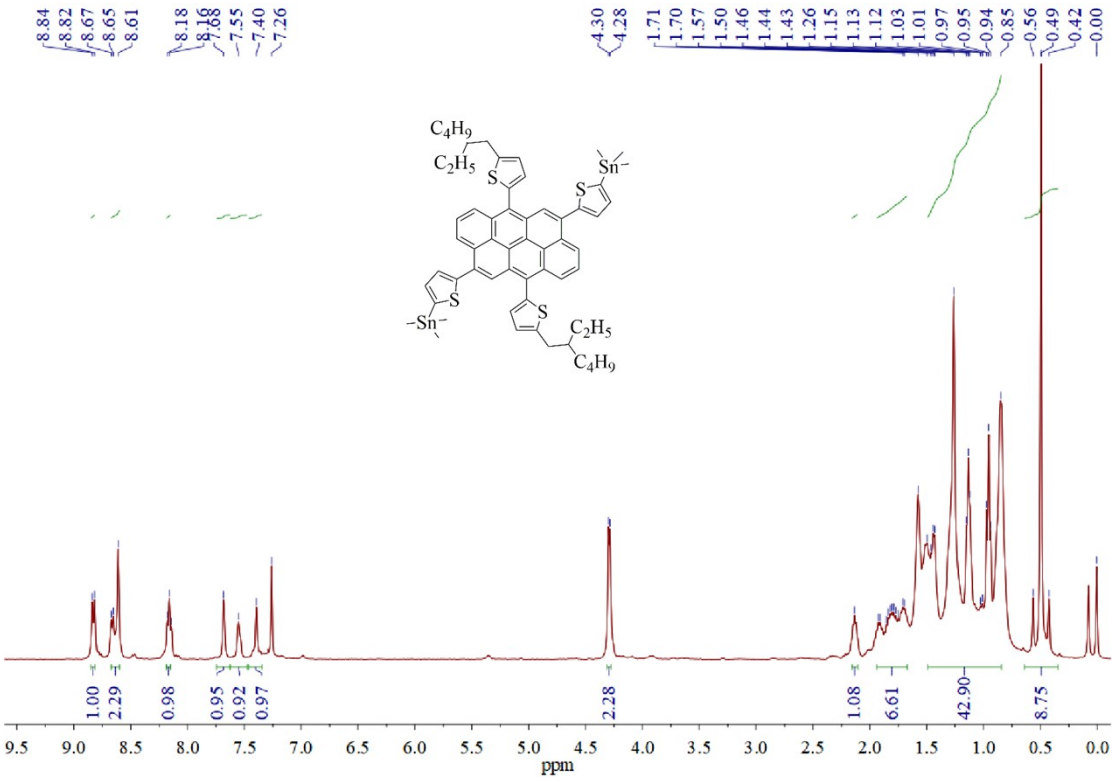

Fig.S6. [1]H NMR spectrum of AANT-T-Sn.

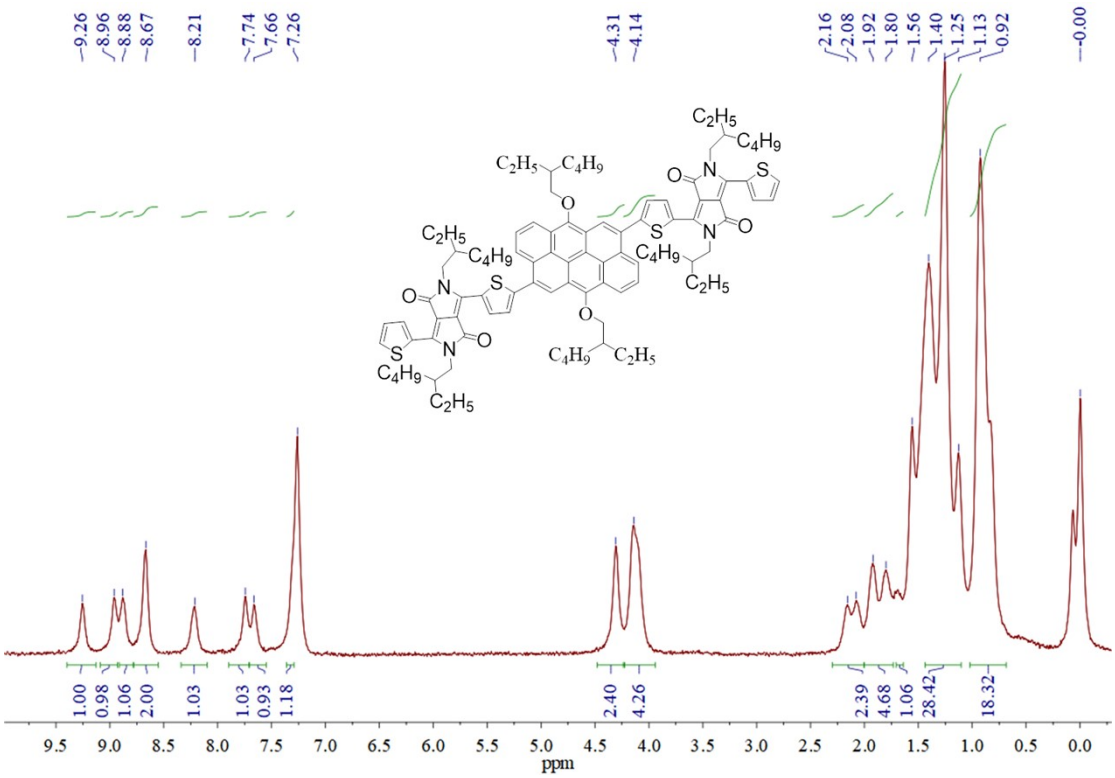

Fig.S7. ^{1}H NMR spectrum of AAN-DPP$_2$.

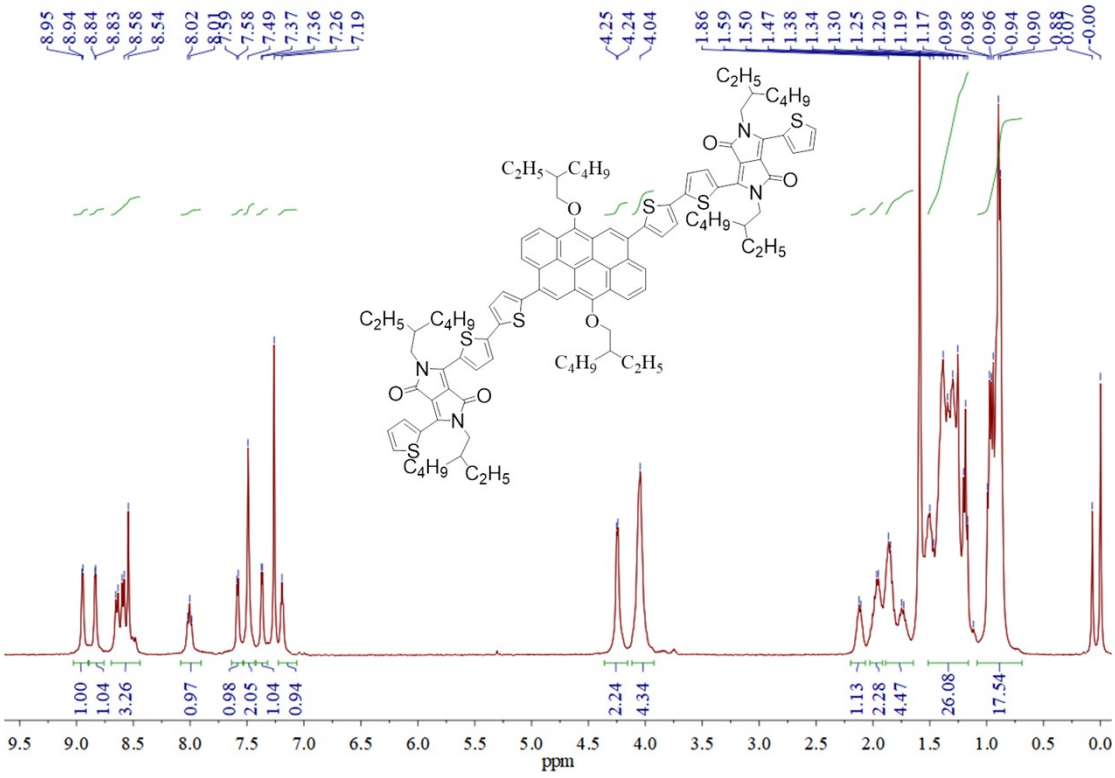

Fig.S8. ^{1}H NMR spectrum of AAN(T-DPP)$_2$.

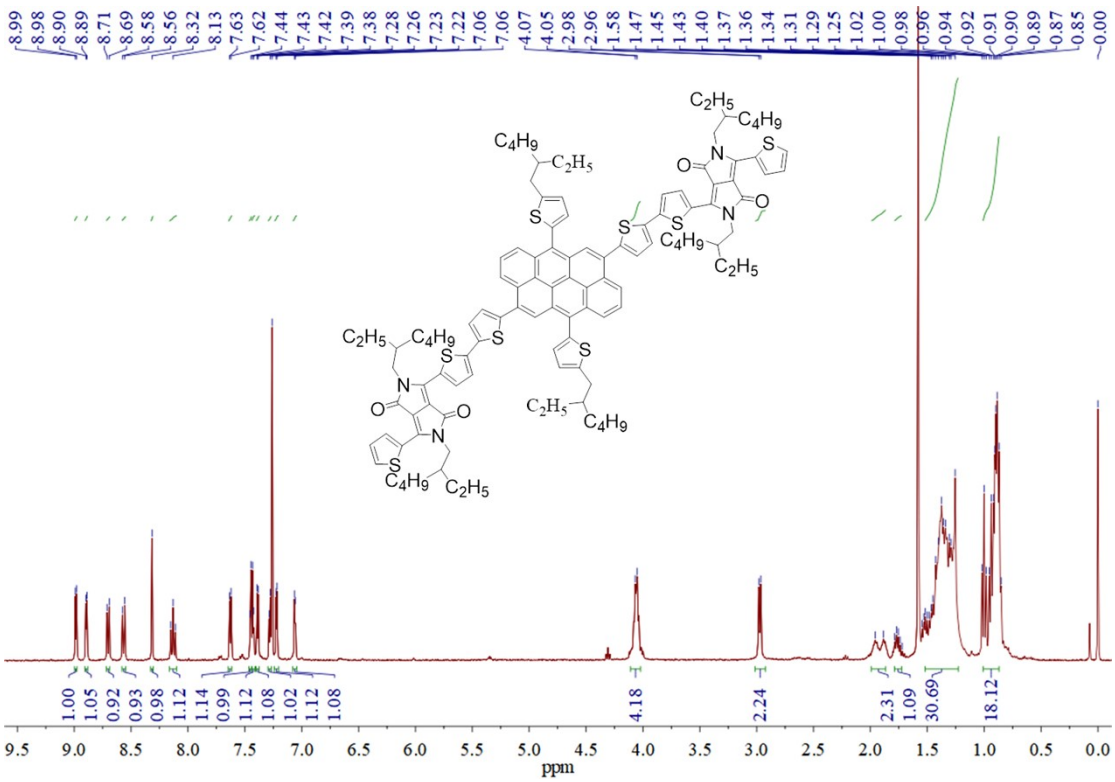

Fig.S9. ^{1}H NMR spectrum of AANT(T-DPP)$_2$.

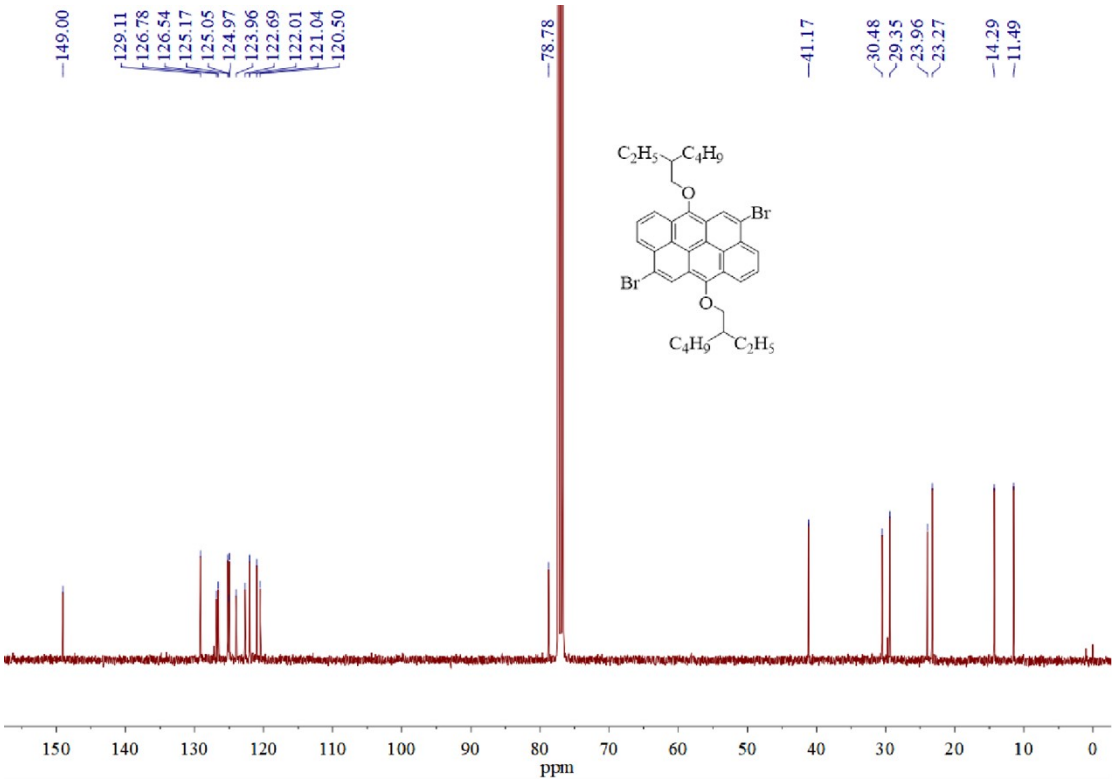

Fig. S10. ^{1}H-NMR spectrum of AAN.

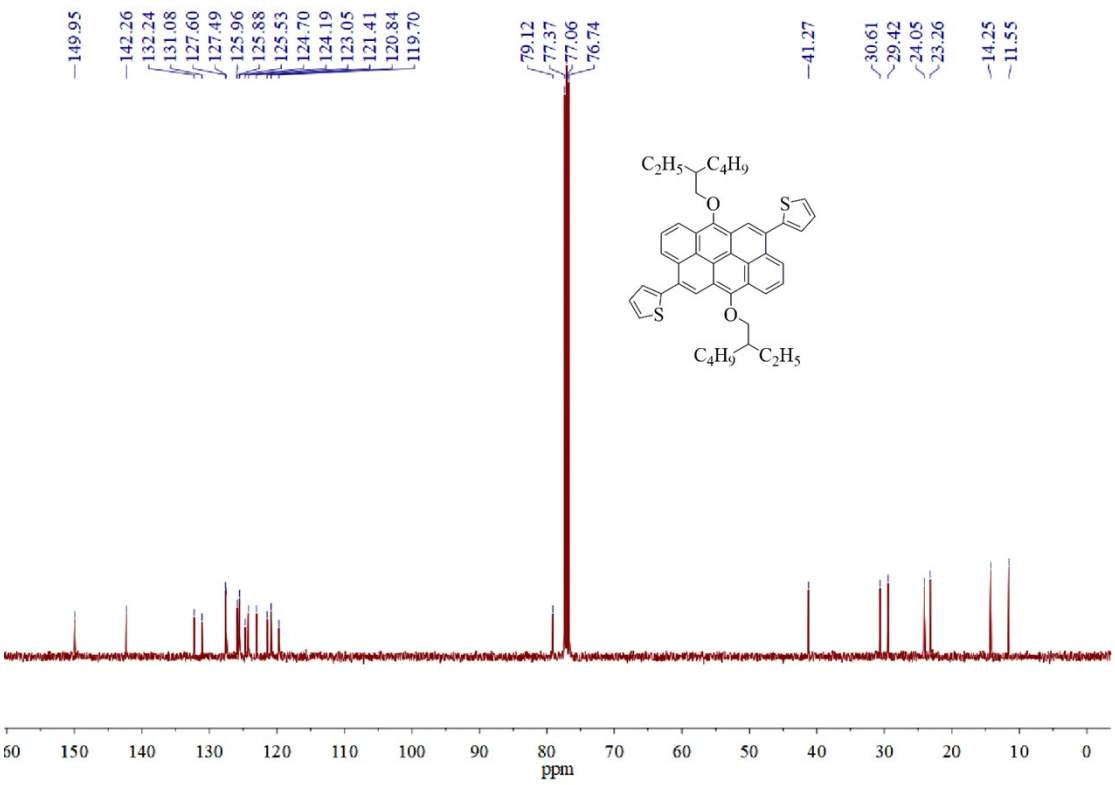

Fig. S11. [1]H-NMR spectrum of AAN-T.

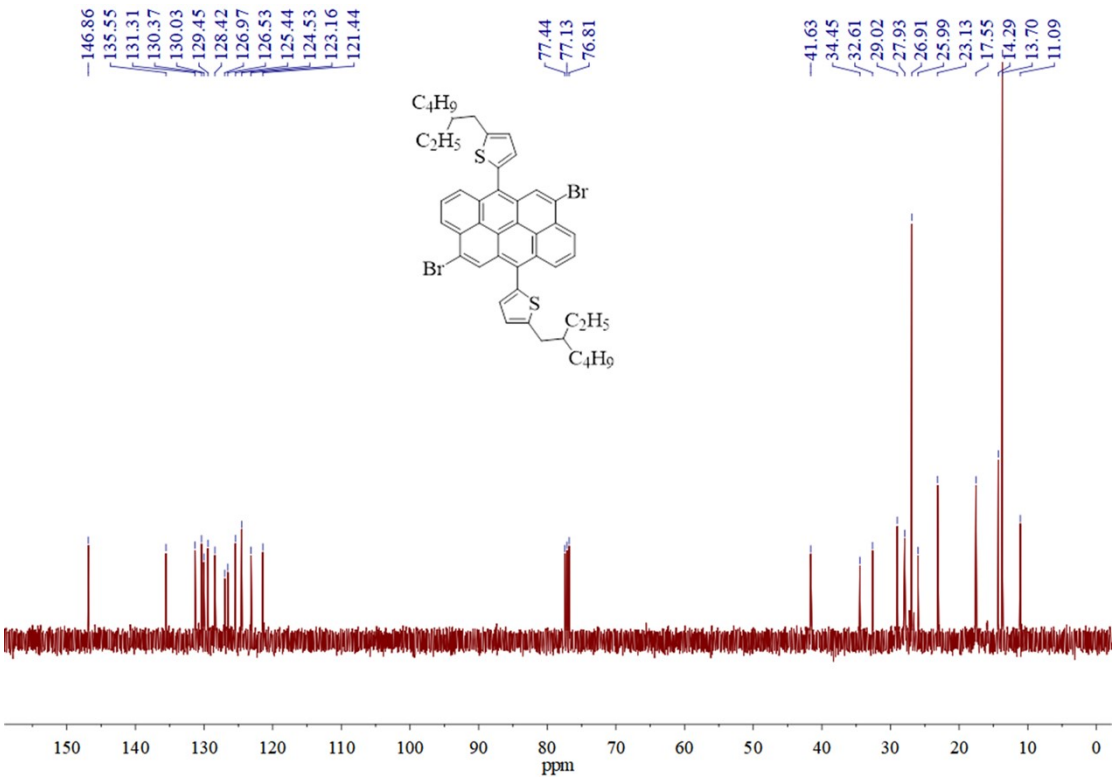

Fig. S12. [1]H-NMR spectrum of AANT.

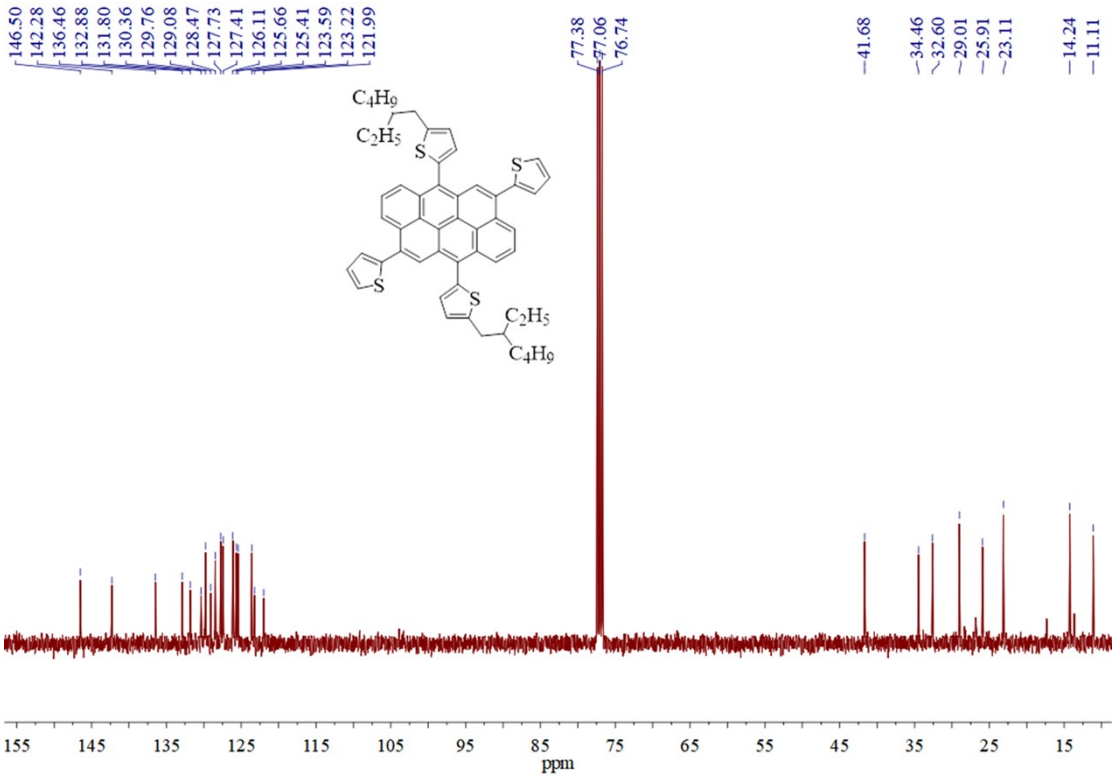

Fig. S13. [1]HNMR spectrum of AANT-T.

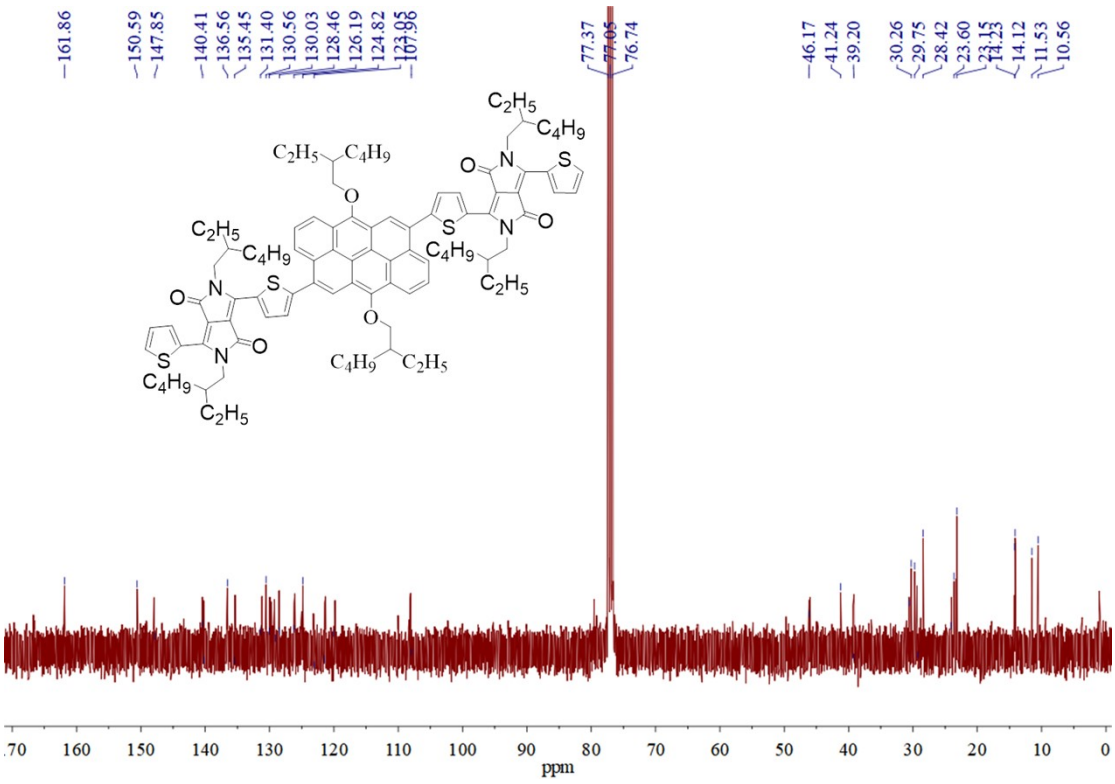

Fig. S14. [1]H-NMR spectrum of AAN-DPP_2.

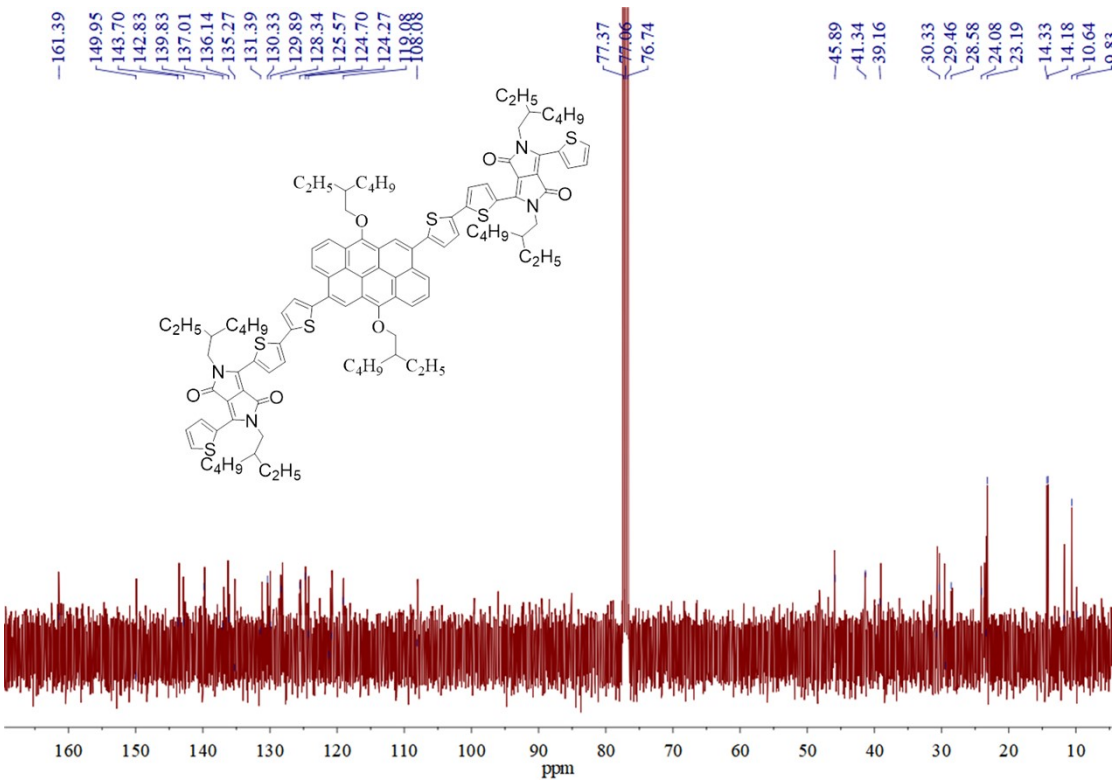

Fig. S15. ^{1}H-NMR spectrum of AAN(T-DPP)$_2$.

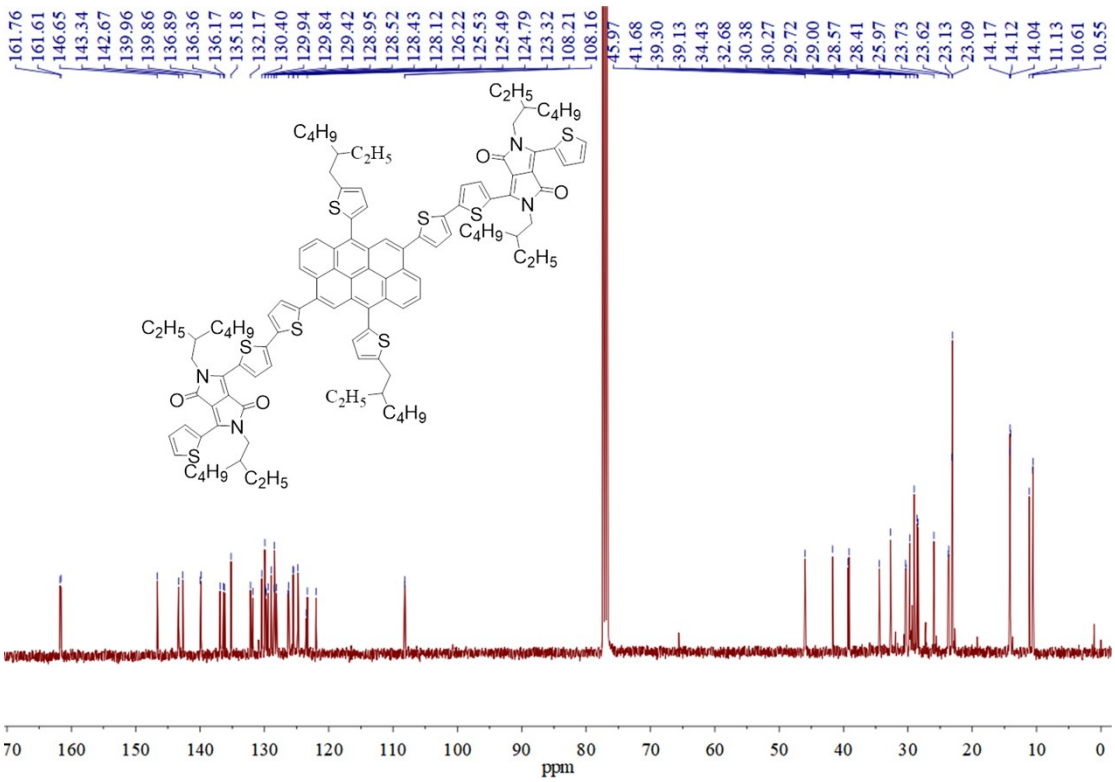

Fig. S16. ^{1}H-NMR spectrum of AANT(T-DPP)$_2$.

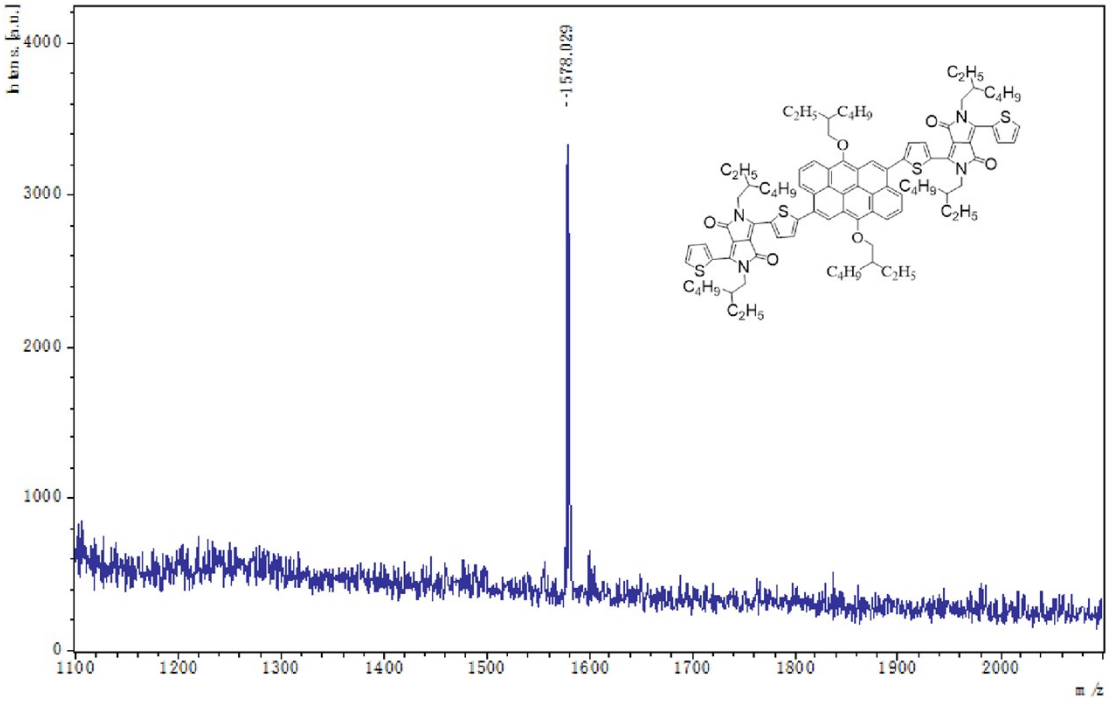

Fig. S17. MALDI-TOF MS Spectrum of AAN-DPP_2.

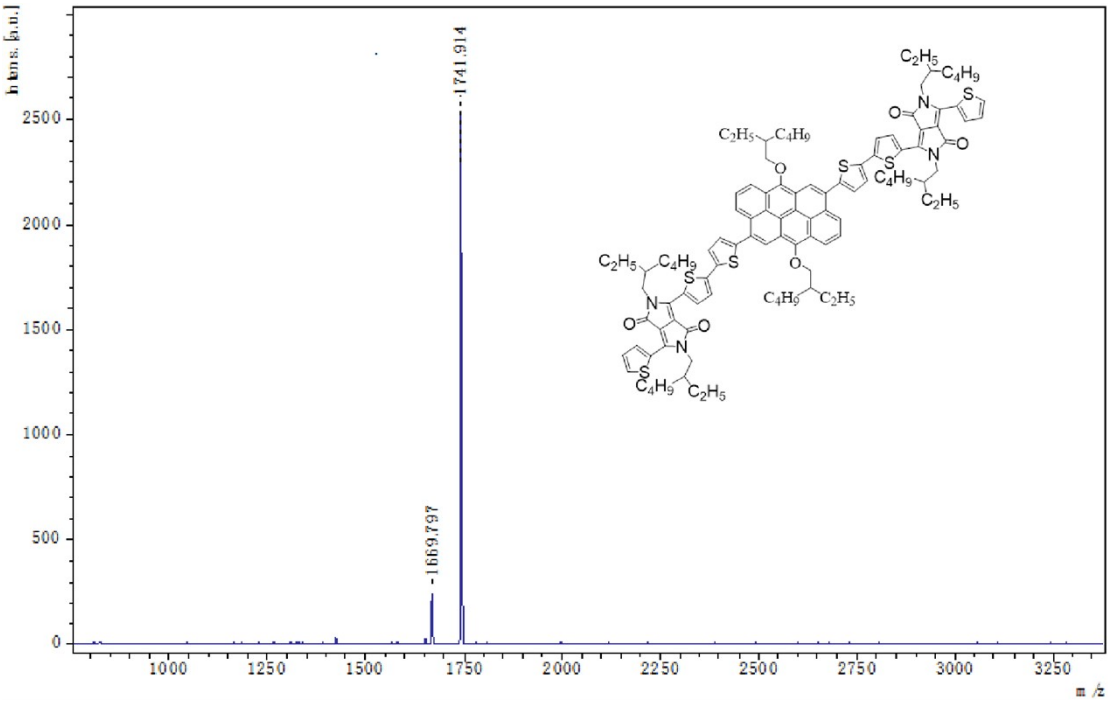

Fig. S18. MALDI-TOF MS Spectrum of AAN(T-$DPP)_2$.

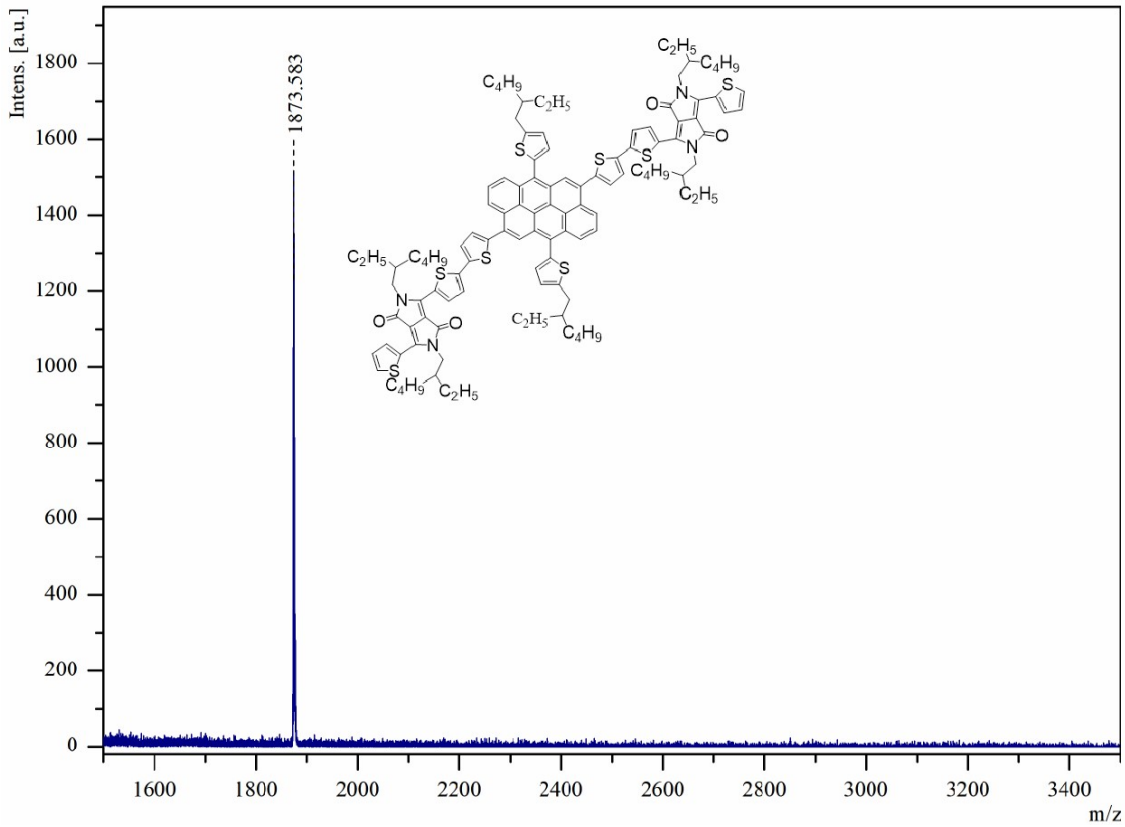

Fig. S19. MALDI-TOF MS Spectrum of AANT(T-DPP)$_2$.

3.The absorption molar coefficient in solution.

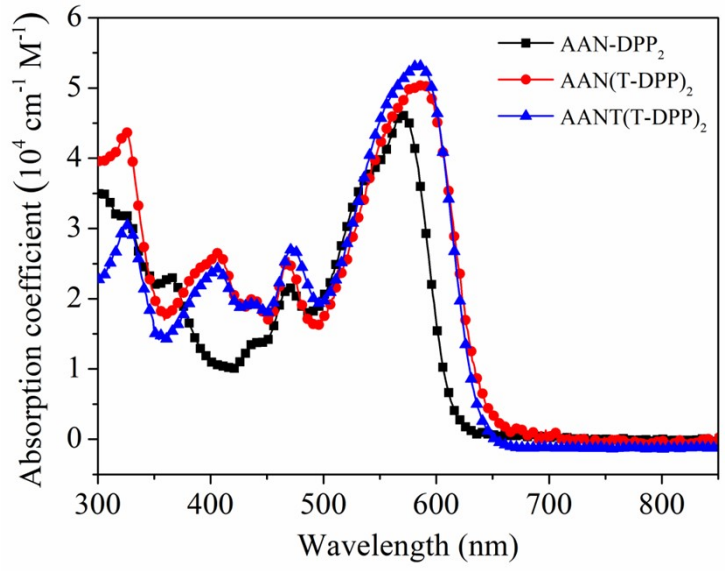

Fig.S20. Absorption spectra of SMs in dilute $CHCl_3$, respectively.

4.Fabrication and Characterization of Organic Solar Cells

A sandwich structure of: ITO/PEDOT:PSS(5000 rpm, 140 ℃ 30min)/SM:$PC_{71}BM$ /Ca (10 nm)/Al (100 nm), was used in the solar cells. The photosensitive layer was subsequently prepared by spin-coating rate of 5000 rpm, with a solution of the SM/$PC_{71}BM$ (1:4, *w/w*) for AAN-DPP_2, (1:3, *w/w*) for AAN$(T\text{-}DPP)_2$ and (1:4, *w/w*) for AANT$(T\text{-}DPP)_2$, respectively. Being dissolved in chloroform (CF) without additive on the PEDOT:PSS layer with a typical concentration of 12 mg mL^{-1} for AAN-DPP_2, AAN$(T\text{-}DPP)_2$, and 10 mg mL^{-1} for AANT$(T\text{-}DPP)_2$. Furthermore, followed by annealing at 70 ˚C for 3 minutes. Ca (10 nm) and Al (100 nm) were successively deposited on the photosensitive layer in vacuum and used as top electrodes. The current-voltage (*I–V*) characterization of the devices was carried out on a computer-controlled Keithley source measurement system. A solar simulator was used as the light source and the light intensity was monitored by a standard Si solar cell. The active area was 0.1 cm^2 for each cell. The thicknesses of the spun-cast films were recorded by a profilometer (Alpha-Step 200, Tencor Instruments). The external quantum efficiency (*EQE*) was measured with a Stanford Research Systems model SR830 DSP lock-in amplifier coupled with WDG3 monochromator and a 150 W xenon lamp.

5. Photovoltaic properties of the AAN-DPP_2/$PC_{71}BM$-based OPV cells.

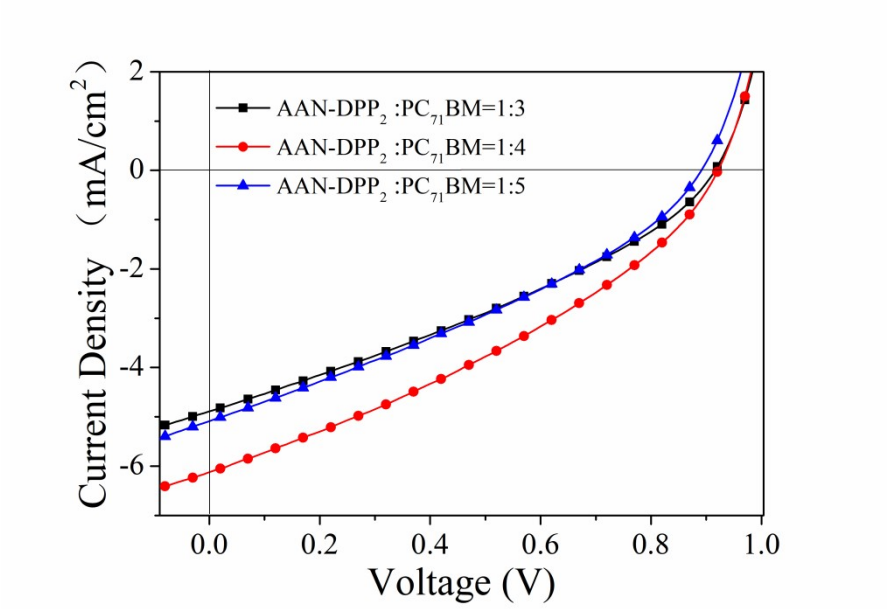

Fig. S21. *J-V* curve of the AAN-DPP_2/$PC_{71}BM$-based OSCs under AM.1.5G illumination (100 mW/cm^2) with SM/$PC_{71}BM$ weight ratios optimization.

Table S1. Photovoltaic parameters of the AAN-DPP_2/$PC_{71}BM$-based OSCs under AM.1.5G illumination (100 mW/cm^2) with SM/$PC_{71}BM$weight ratios optimization.

D/A	V_{oc}(V)	J_{sc}(mA/cm^2)	FF(%)	PCE(%)
1:3	0.91	4.89	32.78	1.46
1:4	0.92	6.12	34.25	1.92
1:5	0.89	5.09	32.67	1.47

Device condition:
(1) chloroform(CF)；
(2) concentration: 12 mg/mL of AAN-DPP_2 in CF;
(3) Structure: ITO/PEDOT:PSS (5000 rpm, 140 ℃, 30 min)/SM:$PC_{71}BM$ (5000 rpm)/Ca (10 nm)/Al (100 nm)
(4) Spin-coating temperature：at room temperature.

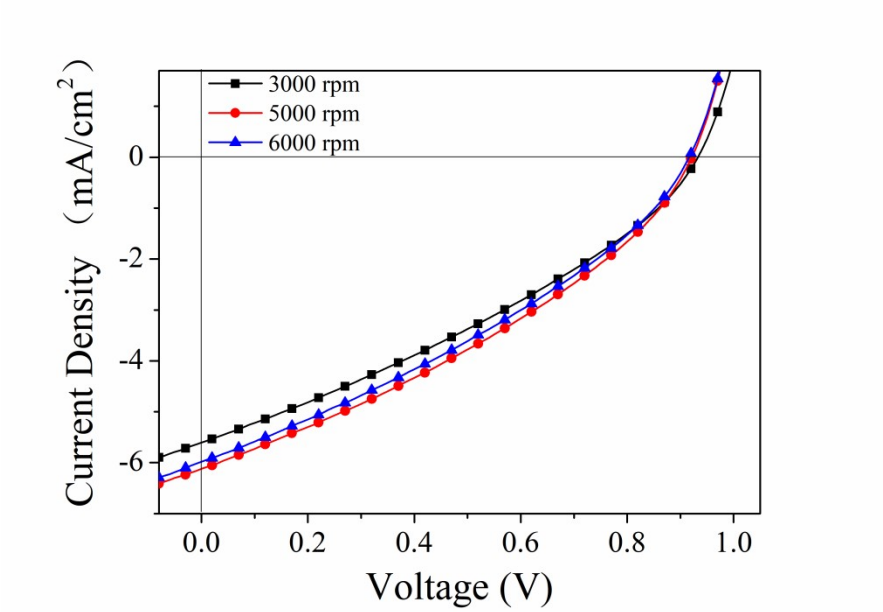

Fig. S22. *J-V* curve of the AAN-DPP_2/$PC_{71}BM$-based OSCs under AM.1.5G illumination (100 mW/cm^2) with SM/$PC_{71}BM$ spin speed optimization.

Table. S2. Photovoltaic parameters of the AAN-DPP_2/$PC_{71}BM$-based OSCs under AM.1.5G illumination (100 mW/cm^2) with SM/$PC_{71}BM$ spin speed optimization.

Spin speed	V_{oc}(V)	J_{sc}(mA/cm^2)	FF(%)	PCE(%)
3000 rmp	0.93	5.60	32.88	1.71
5000 rmp	0.92	6.12	34.25	1.92
6000 rmp	0.91	5.98	33.50	1.82

Device condition:
(1) chloroform(CF)；
(2) concentration: 12 mg/mL of AAN-DPP_2 in CF;
(3) Structure: ITO/PEDOT:PSS (5000 rpm, 140 ℃, 30 min)/SM:$PC_{71}BM$= 1:4/Ca (10 nm)/Al (100 nm)
(4) Spin-coating temperature：at room temperature.

6. Photovoltaic properties of the AAN(T-DPP)$_2$/PC$_{71}$BM-based OPV cells.

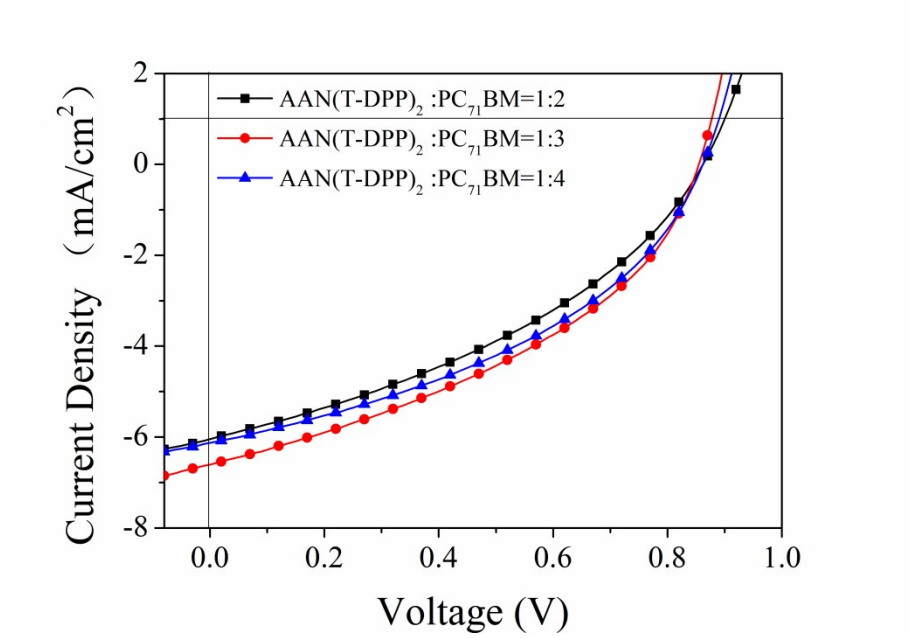

Fig. S23. *J-V* curve of the AAN(T-DPP)$_2$/PC$_{71}$BM-based OSCs under AM.1.5G illumination (100 mW/cm^2) with SM/PC$_{71}$BM weight ratios optimization.

Table. S3. Photovoltaic parameters of the AAN(T-DPP)$_2$/PC$_{71}$BM-based OSCs under AM.1.5G illumination (100 mW/cm^2) with SM/PC$_{71}$BMweight ratios optimization.

D/A	V_{oc}(V)	J_{sc}(mA/cm^2)	FF(%)	PCE(%)
1:2	0.86	6.03	37.85	1.96
1:3	0.85	6.60	40.22	2.26
1:4	0.86	6.12	40.82	2.15

Device condition:
(1) chloroform(CF);
(2) concentration: 12 mg/mL of AAN(T-DPP)$_2$ in CF;
(3) Structure: ITO/PEDOT:PSS (5000 rpm, 140 ℃, 30 min)/SM:PC$_{71}$BM (5000

rpm)/Ca (10 nm)/Al (100 nm)

(4) Spin-coating temperature：at room temperature.

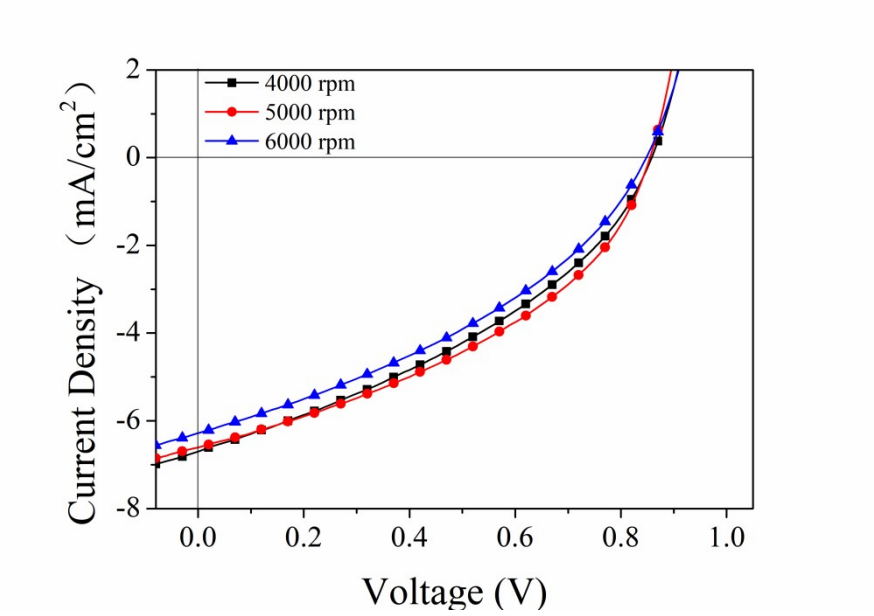

Fig. S24. *J-V* curve of the AAN(T-DPP)$_2$/PC$_{71}$BM-based OSCs under AM.1.5G illumination (100 mW/cm^2) with SM/PC$_{71}$BM spin speed optimization.

Table. S4. Photovoltaic parameters of the AAN(T-DPP)$_2$/PC$_{71}$BM-based OSCs under AM.1.5G illumination (100 mW/cm^2) with SM/PC$_{71}$BM spin speed optimization.

Spin speed	V_{oc}(V)	J_{sc}(mA/cm^2)	FF(%)	PCE(%)
4000 rmp	0.85	6.69	37.29	2.13
5000 rmp	0.85	6.60	40.22	2.26
6000 rmp	0.84	6.27	37.10	1.97

Device condition:

(1) chloroform(CF);

(2) concentration: 12 mg/mL of AAN(T-DPP)$_2$ in CF;

(3) Structure: ITO/PEDOT:PSS (5000 rpm, 140 ℃, 30 min)/SM:PC$_{71}$BM= 1:3/Ca (10 nm)/Al (100 nm)

(4) Spin-coating temperature：at room temperature.

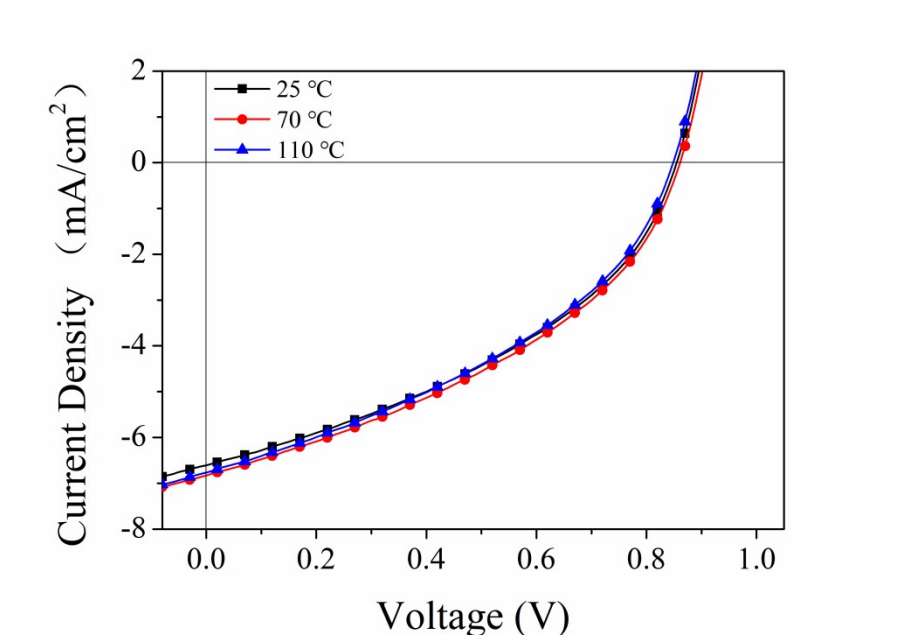

Fig. S25. *J-V* curve of the AAN(T-DPP)$_2$/PC$_{71}$BM-based OSCs under AM.1.5G illumination (100 mW/cm^2) with annealing temperature optimization.

Table. S5. Photovoltaic parameters of the AAN(T-DPP)$_2$/PC$_{71}$BM-based OSCs under AM.1.5G illumination (100 mW/cm^2) with annealing temperature optimization.

Temperature (°C)	**V_{oc}(V)**	**J_{sc}(mA/cm^2)**	**FF(%)**	**PCE(%)**
25	0.85	6.60	40.22	2.26
70	0.86	6.82	39.80	2.33
110	0.85	6.76	39.15	2.24

Device condition:

(1) chloroform(CF)；

(2) concentration: 12 mg/mL of AAN(T-DPP)$_2$ in CF;

(3) Structure: ITO/PEDOT:PSS (5000 rpm, 140 ℃, 30 min)/SM:PC$_{71}$BM= 1:3, 5000 rmp/Ca (10 nm)/Al (100 nm)

7. Photovoltaic properties of the AANT(T-DPP)$_2$/PC$_{71}$BM-based OPV cells.

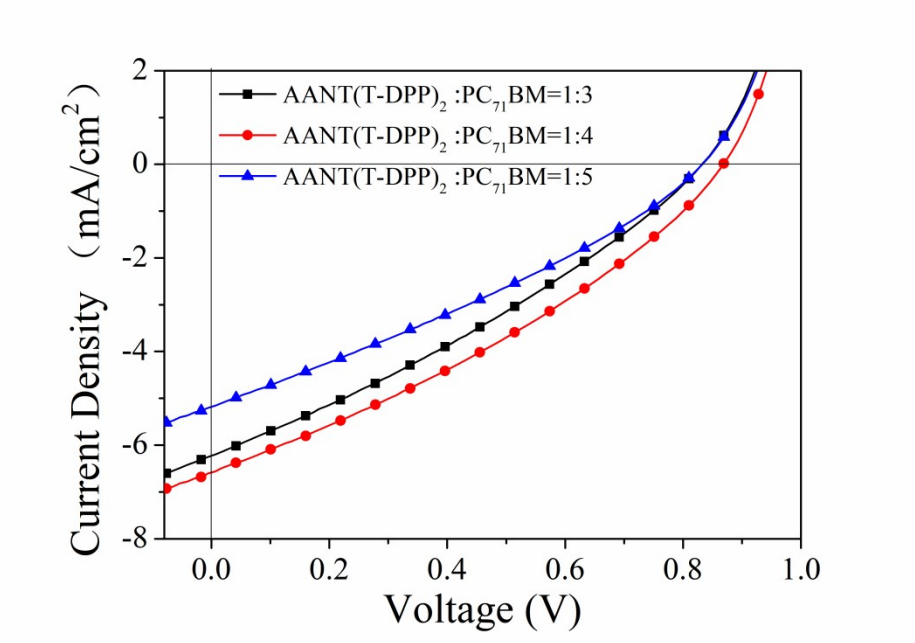

Fig. S26. *J-V* curve of the AANT(T-DPP)$_2$/PC$_{71}$BM-based OSCs under AM.1.5G illumination (100 mW/cm^2) with SM/PC$_{71}$BM weight ratios optimization.

Table. S6. Photovoltaic parameters of the AANT(T-DPP)$_2$/PC$_{71}$BM-based OSCs under AM.1.5G illumination (100 mW/cm^2) with SM/PC$_{71}$BMweight ratios optimization.

D/A	V_{oc}(V)	J_{sc}(mA/cm^2)	FF(%)	PCE(%)
1:3	0.83	6.22	30.82	1.58
1:4	0.86	6.58	32.61	1.85
1:5	0.83	5.18	30.72	1.32

Device condition:

(1) chloroform(CF);

(2) concentration: 12 mg/mL of AANT(T-DPP)$_2$ in CF;

(3) Structure: ITO/PEDOT:PSS (5000 rpm, 140 ℃, 30 min)/SM:PC$_{71}$BM (3000

rpm)/Ca (10 nm)/Al (100 nm)

(4) Spin-coating temperature：at room temperature.

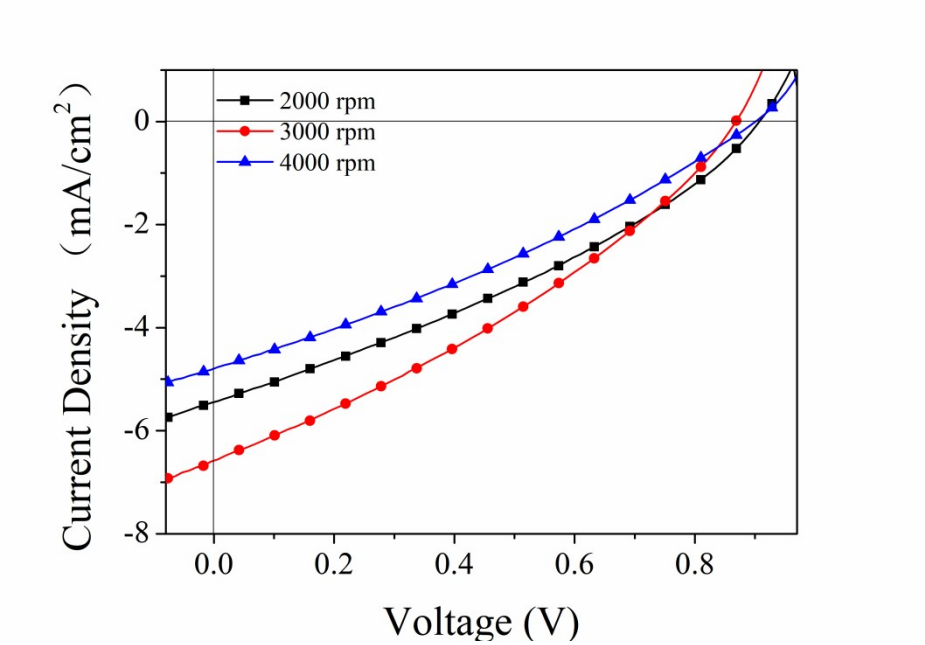

Fig. S27. *J-V* curve of the AANT(T-DPP)$_2$/PC$_{71}$BM-based OSCs under AM.1.5G illumination (100 mW/cm^2) with SM/PC$_{71}$BM spin speed optimization.

Table. S7. Photovoltaic parameters of the AANT(T-DPP)$_2$/PC$_{71}$BM-based OSCs under AM.1.5G illumination (100 mW/cm^2) with SM/PC$_{71}$BM spin speed optimization.

Spin speed	V_{oc}(V)	J_{sc}(mA/cm^2)	FF(%)	PCE(%)
2000 rmp	0.91	5.44	32.48	1.61
3000 rmp	0.86	6.58	32.61	1.85
4000 rmp	0.89	4.79	30.80	1.32

Device condition:

(1) chloroform(CF)；

(2) concentration: 12 mg/mL of AANT(T-DPP)$_2$ in CF;

(3) Structure: ITO/PEDOT:PSS (5000 rpm, 140 ℃, 30 min)/SM:PC$_{71}$BM= 1:4/Ca (10 nm)/Al (100 nm)

(4) Spin-coating temperature：at room temperature.

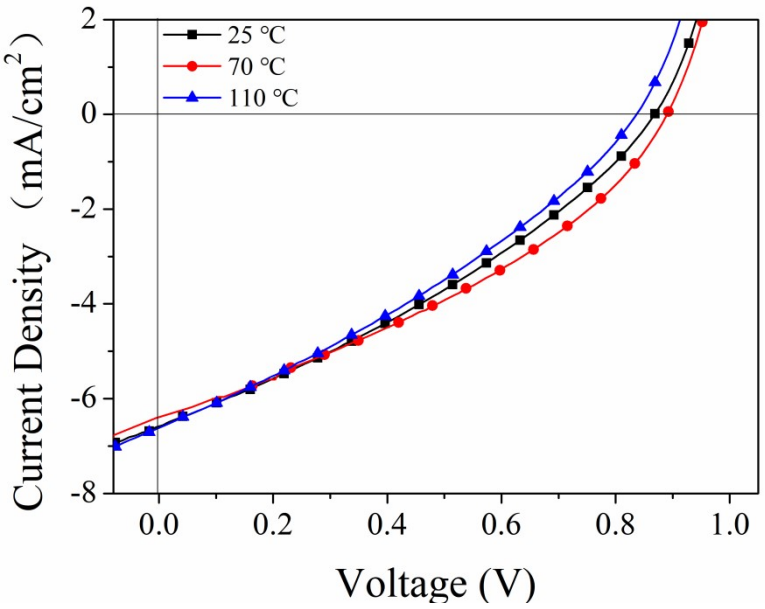

Fig. S28. *J-V* curve of the AANT(T-DPP)$_2$/PC$_{71}$BM-based OSCs under AM.1.5G illumination (100 mW/cm^2) with annealing temperature optimization.

Table. S8. Photovoltaic parameters of the AANT(T-DPP)$_2$/PC$_{71}$BM-based OSCs under AM.1.5G illumination (100 mW/cm^2) with annealing temperature optimization.

Temperature (°C)	V_{oc}(V)	J_{sc}(mA/cm^2)	FF(%)	PCE(%)
25	0.86	6.58	32.61	1.85
70	0.90	6.25	36.12	2.03
110	0.83	6.61	31.87	1.75

Device condition:

(1) chloroform(CF);

(2) concentration: 10 mg/mL of AANT(T-DPP)$_2$ in CF;

(3) Structure: ITO/PEDOT:PSS (5000 rpm, 140 ℃, 30 min)/SM:PC$_{71}$BM= 1:4, 3000 rmp/Ca (10 nm)/Al (100 nm)

8. The PCE distribution of all devices at the optimized conditions.

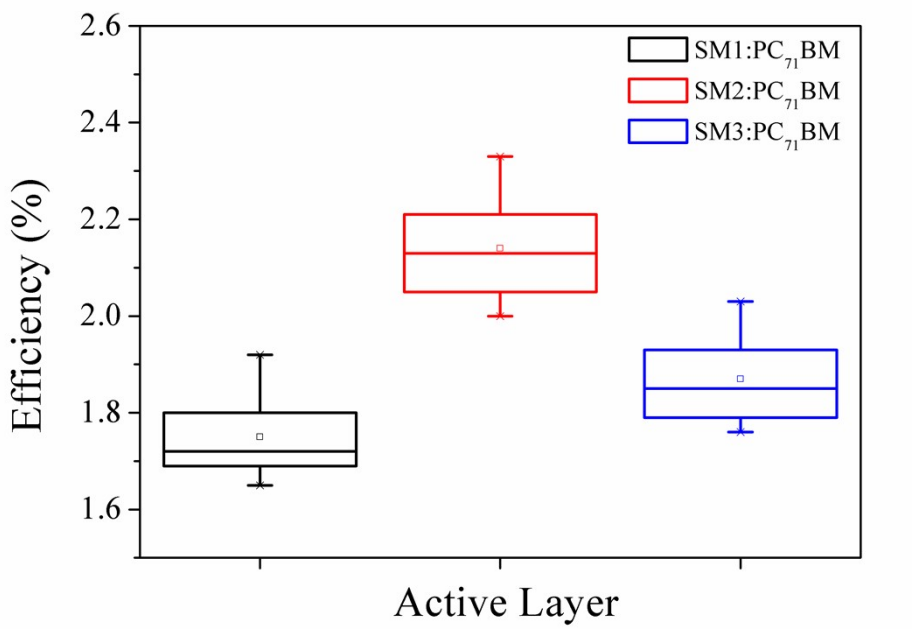

Fig. S29. Efficiency ranges of SM1:$PC_{71}BM$, SM2:$PC_{71}BM$ and SM3:$PC_{71}BM$, respectively. For 10 devices showing minimum, maximum and average efficiency values.